A Multilayer Model for Self-Propagating High-Temperature Synthesis of Intermetallic Compounds

Florence Baras

Laboratoire de Recherches sur la Réactivité des Solides, UMR 5613 CNRS-Université de Bourgogne, 21078 Dijon Cedex, France

Dilip Kondepudi*

Department of Chemistry, Wake Forest University, Winston-Salem, North Carolina 27109

Received: October 15, 2006; In Final Form: February 27, 2007

Self-propagating high-temperature synthesis of intermetallic compounds is of wide interest. We consider reactions in a binary system in which the rise and fall of the temperature during the reaction is such that one of the reacting metals melts but not the other. For such a system, using the phase diagram of the binary system, we present a general theory that describes the reaction taking place in a single solid particle of one component surrounded by the melt of the second component. The theory gives us a set of kinetic equations that describe the propagation of the phase interfaces in the solid particle and the change in composition of the melt that surrounds it. In this article, we derive a set of equations for one- and two-layer systems in which each layer is a binary compound in the phase diagram. The system of equations is numerically solved for Al−Ni to illustrate the applicability of the theory. The method presented here is general and, depending on the complexity of the phase diagram, it could be used to obtain similar equations for systems with more layers.

I. Introduction

Self-propagating high-temperature synthesis (SHS) is an important method for the study and production of intermetallic compounds.[1] The study of kinetics and reaction mechanism of this process is an active field.[2−6] In some studies, the starting specimen is a stack of alternating metal foils of the two metals that react.[7−13] In others, the starting material for this synthesis is a fine powder mixture of two metals,[14] such as Al and Ni or Mo and Si. The powder is compacted into a cylinder, and one end of the cylinder is heated to initiate the reaction. Upon initiation, the exothermic reaction is self-sustaining, and a high-temperature front quickly propagates along the length of the cylinder, converting the metallic powder mixture into intermetallic compounds. The whole process takes only a few seconds or less and is difficult to control. A basic understanding of the relation between the properties of the initial sample and the final product is, therefore, important.

In a binary SHS, depending on the composition and geometry of the compacted sample, the highest temperature reached during the reaction could be below the melting points of the two solids, high enough to melt one but not the other, or high enough to melt both.[1,15] If both components remain solid during the reaction, the reaction rates are slow, and very little of the reactants converts to the product.[16,17] At the other extreme, when both components melt, the mixing of the two fluids through diffusion and convection results in reaction in a liquid phase, and generally, almost complete conversion to the product results.[18,19]

An interesting situation arises in the intermediate case when one of the components, say B, melts and surrounds the solid particles of the other component, say A. In this case, initially A dissolves in B and, as the liquid B diffuses thorough the solid, layers of intermetallic products can form and propagate inward, converting the solid particles of A into the product.[12,14] At the same time, the outermost surface may slowly dissolve into the melt. For example, in the Al−Ni system,[20] Al melts at 933 K and surrounds the Ni particles, whose melting point is 1728 K. If the temperature, *T*, of the reaction does not exceed the melting point of Ni, the formation of the intermetallic compounds is due to liquid/solid reaction. Our goal is to formulate a theory that will describe such reactions taking into account the details and complexity of the reaction on the basis of the phase diagram of the binary system. As the reaction progresses, various intermetallic compounds of the two metals form as intermediate phases. Such layers have been observed in experiments with metal foils[12] and with powders.[14] Our model seeks to describe the dynamics of the growth of these layers and to predict the final multilayer structure of a typical particle. This structure is, of course, related to the particle size and the temperature variation it is subjected to during the reaction.[14]

Several theoretical approaches to modeling reactions between solid particles in a melt have been proposed. Following the mechanistic studies of Aleksandrov and Korchagin,[21] a model for describing the reaction of carbon particles in a melt of was proposed by Kanury.[22] In this model, a layer of intermetallide Ti−C compound forms around the carbon particle. The Ti atoms diffuse across this layer and react with the solid carbon core and convert it to the intermetallide. At the same time, at its outer surface, the intermetallide layer dissolves into the melt, increasing the amount of TiC in the molten Ti. It is assumed that the thickness of the intermetallide layer across which the Ti atoms diffuse reaches a steady state and remains constant. Under these conditions, Kanury's theoretical model describes the time evolution of the C particles and the composition of

* Corresponding author. E-mail: dilip@wfu.edu.

10.1021/jp066776p CCC: $37.00
Published on Web 05/18/2007

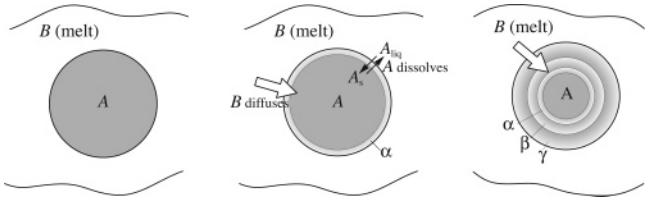

Figure 1. Different stages of the reaction mechanism between two metals, A and B. The highest temperature the system reaches is higher than the melting point of B but lower than the melting point of A. (a) At the start, B melts and surrounds particles of A. (b) During the next stage, A begins to dissolve in B and at the same time, B diffuses into particles of A. (c) As B diffuses into A, successive layers of intermetallic compounds, α, β, γ, form while the outermost layer, γ, dissolves into the melt.

the melt. Along similar lines, Hibino[23] developed a model for the Ni−Al system in which molten Al surrounds Ni particles. In this case, a layer of the intermetallic compound Ni_2Al_3 forms around the Ni particle. Al from the liquid diffuses through the Ni_2Al_3 layer toward the Ni_2Al_3/Ni interface and reacts with Ni to produce Ni_2Al_3, thus increasing the thickness of the Ni_2Al_3 layer. Hibino[23] used the model to obtain the rate at which heat is evolved in the exothermic reaction and to describe propagation of the high-temperature front. The theoretical model of Gennari et al.[24−29] also considers the Al−Ni system and models the product formation in terms of the diffusion controlled dissolution of solid Ni particles into liquid Al and predicts the spatiotemporal evolution of the temperature of the system.

In the model presented below, we take a different approach. Our focus is on a "typical" single solid particle surrounded by a liquid. The whole system is subjected to a propagating temperature front. The time evolution of the temperature, *T*, is assumed to be given; it is the temperature a typical particle in the system experiences. Our goal is the prediction of the time evolution of the layered structure of the particle for a given temperature front. On the spatial scale of the particle, the temperature can be assumed to be uniform. We consider binary systems with components A and B that can react to form compounds α, β, ..., etc. The reaction proceeds through the following stages (see Figure 1):

- First, component B melts and surrounds particles of A, which are assumed to be spherical for simplicity, but other shapes could also be considered. (Minimization of interfacial energy at high temperatures may drive the particles to be spherical.)
- Next, particle A begins to dissolve into liquid B, and at the same time, B diffuses into A and forms a layer of intermetallic compound, say α.
- Since the A/α interface is not in equilibrium, driven by the diffusion of B (more accurately, interdiffusion of A and B) through the α layer, more of A converts to α. Thus, the thickness of the α layer grows.
- At the outer surface of the α layer, B may react with the α phase to produce another intermetallic compound β, resulting in the growth of a β layer. Similarly, more layers, γ, δ, etc., could form successively, depending on the number of compounds that the components A and B can form.
- The outermost layer dissolves into the melt, thus changing the composition of the melt.

To elucidate the basic formalism of the above model, we begin with the simple case of a one-layer model, in which there is only one significant intermetallic compound that forms. Then, we extend the model to a two-layer model in which two intermetallic compounds form. Through this discussion, the generalization of this method to more layers would be made clear.

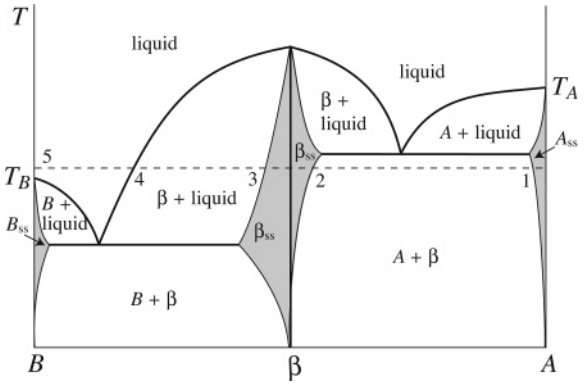

Figure 2. Phase diagram for binary system of A and B forming a intermetallic compound β. The path from point 1 to point 2 represents the diffusion of molten B into the sphere A, resulting in compound formation with composition corresponding to the point 2.

II. Single-Layer Model

The two metals of the binary system are denoted by A and B. In this model, we assume only one intermetallic compound, BA, which we denote by β, can form during the reaction. A possible phase diagram associated with such an A−B binary system is shown in Figure 2. In this diagram, we included small regions in which the system is a solid solution of A and β or B and β to illustrate their effect on the product. As we shall see below, these solid−solution phases will be a part of the layered structure into which A will transform due to the reaction. If these solid−solution parts of the phase diagram are very narrow, they can be ignored as a first approximation, but we include them in our modeling.

As in the case of SHS reactions, we assume a mixture of fine particles of A and B compacted into a cylinder. This cylinder is heated at one end to initiate the reaction. Upon initiation, the exothermic reaction generates sufficient heat to sustain the reaction, and a high-temperature front quickly propagates along the length of the cylinder. The temperature of the front is high enough to melt B but not A. The formation of the intermetallic compound begins when component B melts and surrounds particles of A and the reaction proceeds as outlined in the previous section. Each particle of A is, thus, subjected to a temperature front and is surrounded by the melt of B. The consequent transformation of the structure of A is the focus of our model. The model describes the time evolution of a typical particle for a specified variation of the temperature, *T*.

As generally in SHS, the temperature increases, reaches a maximum value, and slowly decreases. The maximum value reached depends on the exothermicity, the particle size, and the density of the reacting sample.[1,14] A typical temperature profile in SHS is shown in Figure 3. The increase in *T* is approximated by the expression

$$T(t) = T_0 + \frac{C\exp(ct)}{D + \exp(dt)} \tag{1}$$

which captures the main features of the thermogram observed experimentally.[16,23,30−33] Once *T* reaches its maximum value, which depends on the sample and the initial heating rates, it begins to decrease due to heat losses. In our modeling, we assume a mean temperature field that each particle of A, and the molten A that surrounds it, is subjected to is given by a profile shown in Figure 3.

At temperatures below the melting point of B, when both components are solids, the reaction rate is virtually zero.[16,17]

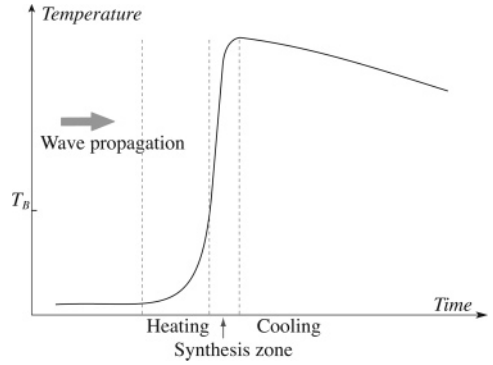

Figure 3. A typical temperature profile in SHS synthesis. It is the mean T variation each particle in the reacting sample is subjected to.

When T exceeds the melting temperature of B, the reaction begins. At the initial stage, solid A begins to dissolve in liquid B,[14] and at the same time, liquid B begins to diffuse into solid A at a significant rate because the temperature is high enough (we shall describe interdiffusion of A and B as diffusion of B in A). As implied by the phase diagram, due to the diffusion of B, a solid solution of B in A forms until the point "1" in Figure 2 is reached. At that point, the reaction

$$\mathrm{A} + \mathrm{B} \rightleftharpoons \beta \tag{2}$$

begins to take place at the interface, forming a layer of the compound phase β, at which point there is no direct contact between solid A and the liquid phase. In our model, the β layer in contact with the liquid phase can dissolve into the liquid phase. We assume that the dominant mechanism through which A enters the liquid phase is the dissolution of β layer, whereas a relatively small amount of A might diffuse through the β layer. Accordingly, we ignore the diffusion of A through the β layer and only include the dissolution of β in our model. At this stage, a small part of A would have dissolved into liquid B to form a dilute solution. By referring to the phase diagram, we assume the mole fraction of A in the solution is not high enough for the formation a solid phase, that is, the composition of the liquid to the left of point 4 in Figure 2. The mole fraction of A in the solution when a layer of β forms will be taken as an initial condition in our model; its value is to be determined through an analysis of the dissolution process and as such is not a prediction of the model. However, the composition of the melt does change in the model because the outermost layer, in this case, β, also dissolves into the melt, thus enriching the melt in A. The final composition of the melt depends on this dissolution rate.

Figure 4 summarizes the processes occurring at different locations in the system. The reaction 2 takes place at the interface, I, at a rate R_1. The rate of reaction 2, R_1(mol m^{-2} s^{-1}), in the first approximation could be taken to be proportional to the $(a_1 - a_{1,\mathrm{eq}})$ in which a_1 is the activity of B at the interface, I, and $a_{1,\mathrm{eq}}$ is its equilibrium value when reaction 2 is considered. The equilibrium value of $a_{1,\mathrm{eq}}$ is obtained using $\mu_\mathrm{A} + \mu_\mathrm{B} = \mu_\beta$, in which μ's are the chemical potentials. From basic thermodynamics of irreversible processes,[34] it follows that, for small deviations from equilibrium, the rate of reaction is proportional to the affinity $\mathcal{A} = \mu_\mathrm{A} + \mu_\mathrm{B} - \mu_\beta$. The chemical potential of x can be written as

$$\mu_x = \mu_x^0 + RT \ln a_x$$

in which a_x is the activity and μ_x^0 is the standard-state chemical potential. Noting that the chemical potentials of pure A and the

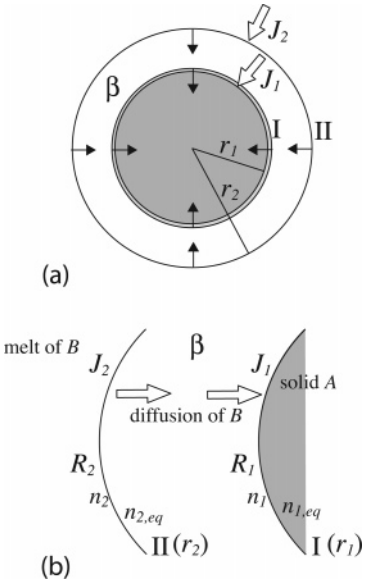

Figure 4. (a) Physical description of the solid-state reaction in which one layer of the intermetallic compound β forms as the molten compound B diffuses through the solid sphere of A. (b) Kinetic details of the model. J_1 is the diffusion current of B at the interfaces I, which are balanced by the reaction $\mathrm{A} + \mathrm{B} \rightleftharpoons \beta$, which occurs at the rate R_1. J_2 is the current at interface II. At interface II, β dissolves into the melt B at rate R_2. n_1 and n_2 are the mole fractions of B, whose equilibrium values are specified by the subscript "eq".

major component β in the β-phase do not change as much as the chemical potential of the minor component B in the β-phase, one can easily see that, close to equilibrium, for the reaction $\mathrm{A} + \mathrm{B} \rightarrow \beta$, the affinity is proportional to $(a_1 - a_{1,\mathrm{eq}})$. Since the rate of a reaction close to equilibrium is proportional to the affinity, we can write the rate R_1 at the interface, I, as $R_1 \sim k_1(a_1 - a_{1,\mathrm{eq}})$. The activity, a_1, is equal to $\gamma_\mathrm{k} n_\mathrm{k}$ in which n_k is the mole fraction and γ_k is the activity coefficient, which for ideal systems equals 1. In order to simplify the theory, we shall assume $\gamma_\mathrm{k} \sim 1$. Thus, the rate of reaction at the interface is assumed to be

$$R_1 \sim k_1(a_1 - a_{1,\mathrm{eq}}) \sim k_1(n_1 - n_{1,\mathrm{eq}}) \tag{3}$$

in which k_1 is the T-dependent rate constant: $k_1 = k_{10} \exp(-E_1/RT)$. Such an approximation is not a major limitation of the theory. For the development of our theory, we only require that the reaction rate R_1 be expressed as a function of the mole fractions of the various components. The above approximation is made only to simplify the discussion; it is not a limitation of the theory. As the reaction progresses, A is converted to β, and the layer of β begins to propagate inward, as shown in Figure 4. At the reaction interface, I, composition of the β-layer corresponds to point 2 shown in Figure 2. The reaction rate, which is very rapid at high temperatures, quickly reaches a value at which it balances the diffusional flow, J_1, of B at interface I, thus maintaining a quasi-steady state. This implies

$$J_1 = R_1 \tag{4}$$

(This equation does not mean that the diffusional flow is zero if there is no formation of the compound β; interdiffusion of A and B will occur whether or not a compound is formed.) At this stage, B continues to diffuse from the solution through the β-layer, forming a solid solution, consistent with the phase diagram. At steady state, the total diffusional flux of B at the

interface II (Figure 4), must balance the total flux at surface I. This leads to the condition

$$r_2^2 J_2 = r_1^2 J_1 \tag{5}$$

For spherical geometry, writing the diffusion equation in spherical coordinates, one can easily show[35] (see the Appendix) that the steady-state current can be expressed in terms of mole fraction, n, of B at the boundaries. This leads to the relation

$$J_1 = W_{12}(n_2 - n_1) \tag{6}$$

with

$$W_{12} = D_1 \frac{r_2}{r_1} \frac{1}{r_2 - r_1}$$

in which D_1 is the diffusion coefficient of B in the β-phase, and n_1 and n_2 are the mole fractions of B at interfaces I and II. In the above expressions, following thermodynamic formulation of diffusion, the diffusion current is expressed as the gradient of the mole fraction, not a gradient of concentration, as in Fick's law. As shown in Section IV, for small values of the mole fraction, it is easy to see that $D_1 = D_{1N}/V_m$ in which D_{1N} is the Fick's-law diffusion coefficient (units $m^2\ s^{-1}$) and V_m is the molar volume of the phase in which the diffusion of a compound is taking place. The units of D_1 are mol $m^{-1}\ s^{-1}$. We assume the diffusion coefficient has an Arrhenius temperature dependence: $D_1 = D_{10} \exp(-\epsilon_1/RT)$.

At interface II, we assume β dissolves in B to form a solution in accordance with the phase diagram. We denote this by the "reaction"

$$\beta \rightleftharpoons \text{melt} \tag{7}$$

We can assume that the rate of dissolution is given by

$$R_2 = k_2(n_2 - n_{2,eq}) \tag{8}$$

k_2 being an Arrhenius rate constant: $k_2 = k_{20} \exp(-E_2/RT)$. Note that this form is consistent with a dissolution rate that depends on diffusion with Arrhenius temperature dependence.

With the processes as described above, we are now in a position to write the rate equations of the system using the following variables:

N'_B = amount (moles) of B in the melt
N'_A = amount (moles) of A in the melt
N_β = amount (moles) of β
N_A = amount (moles) of pure A in the inner sphere
V_{mA} = molar volume of solid A
$V_{m\beta}$ = molar volume of $\beta \sim 2V_{mA}$
V_{mB} = molar volume of liquid B
a_1 = activity of B at surface I $\sim n_1$ = mole fraction at surface I
$a_{1,eq}$ = equilibrium activity of B at surface I $\sim n_{1,eq}$ = equilibrium mole fraction at surface I
a_2 = activity of B at surface II $\sim n_2$ = mole fraction at surface II
$a_{2,eq}$ = equilibrium activity of B at surface II $\sim n_{2,eq}$ = equilibrium mole fraction at surface II
D_1 = diffusion coefficient of B in the β phase
J_1 = diffusion current at surface I
J_2 = diffusion current at surface II
R_1 = reaction rate at surface I
R_2 = reaction rate at surface II

Considering reactions at the interfaces, the equations for the amounts (moles) of each substance are

$$\frac{d}{dt}N_A = -4\pi r_1^2 R_1 \tag{9a}$$

$$\frac{d}{dt}N_\beta = 4\pi r_1^2 R_1 - 4\pi r_2^2 R_2 \tag{9b}$$

$$\frac{d}{dt}N'_B = 4\pi r_2^2(-J_2 + R_2) = 4\pi r_2^2 R_2 - 4\pi r_1^2 R_1 \tag{9c}$$

$$\frac{d}{dt}N'_A = 4\pi r_2^2 R_2 \tag{9d}$$

where we have used steady-state assumption 4 and 5 in eq 9c. Conservation of A and B implies

$$\frac{d}{dt}(N_A + N_\beta + N'_A) = 0$$

and

$$\frac{d}{dt}(N_\beta + N'_B) = 0$$

It is easy to see that eqs 9a−d satisfy these conservation equations.

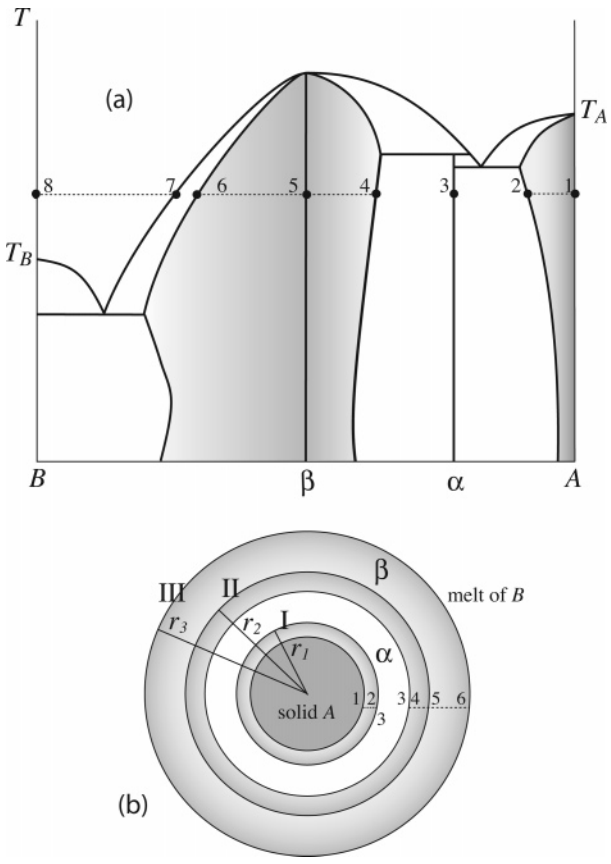

Figure 5. (a) Phase diagram of a binary system with two compounds, α and β. (b) The sphere with layers of intermetallic compounds α and β. The dashed lines correspond to the dashed lines 1−2 and 4−6 in the phase diagram. The β phase is a solid solution of variable composition.

The above equations can be converted into equations of the time evolution of the surface radii, r_1 and r_2, by noting that

$$N_A = \frac{4\pi}{3} r_1^3 \frac{1}{V_{mA}}$$

and

$$N_\beta = \frac{4\pi}{3}(r_2^3 - r_1^3)\frac{1}{V_{m\beta}} \tag{10}$$

Using 10 in 9a and 9b, we obtain

$$\frac{dr_1}{dt} = -V_{mA} R_1 \tag{11}$$

and

$$4\pi\left(r_2^2 \frac{dr_2}{dt} - r_1^2 \frac{dr_1}{dt}\right)\frac{1}{V_{m\beta}} = 4\pi r_1^2 R_1 - 4\pi r_2^2 R_2$$

which simplifies to

$$\frac{dr_2}{dt} = (V_{m\beta} - V_{mA})\frac{r_1^2}{r_2^2} R_1 - V_{m\beta} R_2 \tag{12}$$

The first term on the right-hand side of eq 12 is due to the change in the volume when solid A is converted to β; it vanishes if there is no change in volume. The reaction rate $R_2 = k_1(n_2 - n_{1,eq})$ can be written explicitly in terms of N'_A and N'_B because

$$n_2 = \frac{N'_B}{N'_B + N'_A}$$

This gives us the following set of coupled equations in r_1, r_2, N'_A and N'_B, which we shall call systems variables.

$$\frac{dr_1}{dt} = -V_{mA} R_1 \tag{13a}$$

$$\frac{dr_2}{dt} = (V_{m\beta} - V_{mA})\frac{r_1^2}{r_2^2} R_1 - V_{m\beta} k_2 (n_2 - n_{2,eq}) \tag{13b}$$

$$\frac{d}{dt} N'_B = -4\pi r_1^2 R_1 + 4\pi r_2^2 k_2 (n_2 - n_{2,eq}) \tag{13c}$$

$$\frac{d}{dt} N'_A = 4\pi r_2^2 k_2 (n_2 - n_{2,eq}) \tag{13d}$$

To obtain a set of closed equations, we now show that $R_1 = k_1(n_1 - n_{1,eq})$ can be written in terms of $(n_2 - n_{1,eq})$. To this end, we first note that at steady state,

$$r_2^2 J_2 = r_1^2 J_1 \qquad J_1 = R_1$$

$$J_1 = W_{12}(n_2 - n_1)$$

in which

$$W_{12} = D_1 \frac{r_2}{r_1}\frac{1}{r_2 - r_1} \tag{14}$$

At steady state, since $J_1 = R_1$ at surface I,

$$R_1 = k_1(n_1 - n_{1,eq}) = J_1 = W_{12}(n_2 - n_1) = W_{12}[(n_2 - n_{1,eq}) - (n_1 - n_{1,eq})] \tag{15}$$

From this equation we arrive at

$$(n_1 - n_{1,eq}) = \frac{W_{12}}{k_1 + W_{12}}(n_2 - n_{1,eq})$$

Using this expression, the reaction rate can now be written as

$$R_1 = k_1(n_1 - n_{1,eq}) = \frac{k_1 W_{12}}{k_1 + W_{12}}(n_2 - n_{1,eq}) \tag{16}$$

in which W_{12} is a function of r_1, r_2, and the diffusion coefficient D_1, as shown in eq 14. Thus, R_1 can be written as a function of r_1, r_2, and $n_2 = N'_B/(N'_B + N'_A)$. Combining eqs 14 and 16 with eq 13, we have a complete set of coupled equations for r_1, r_2, N'_A, and N'_B. These are a set of closed, nonlinear equations in r_1, r_2, N'_A, and N'_B. They can be solved numerically to understand the evolution of the system's composition. In solving the above set of equations, the following parameters must be specified: $n_{1,eq}$, $n_{2,eq}$, D_1, k_1, and k_2 (as functions of T), along with initial values. The temperature itself is a function of time $T(t)$. The solutions give the time evolution of the composition of the reacting sphere. If the enthalpies of formation of the β layer and its dissolution into the melt of B are known, the heat generated by the reacting sphere could also be obtained as a function of time.

$R_1 = 0$ when $(n_1 - n_{1,eq}) = 0$; therefore, for small values of $(n_1 - n_{1,eq})$, we assumed that it was a linear function of $(n_1 - n_{1,eq})$. If R_1 is not a linear function of $(n_1 - n_{1,eq})$, the steady-state relation (15), that is, $R_1 = W_{12}(n_2 - n_1)$, could in principle be solved to express n_1 as a function of n_2; thus, R_1 could itself be expressed as a function of $(n_2 - n_{1,eq})$. Substituting R_1 as a function of $(n_2 - n_{1,eq})$ into eqs 13a–d, a closed set of equations for r_1, r_2, N'_A, and N'_B could be obtained.

III. Two-Layer Model

Extending the model presented in the previous section to the case of the system that can form two compounds, α and β, is straightforward. A possible binary phase diagram that has two compounds, α and β, is shown in Figure 5. This phase diagram approximates the Ni–Al binary for temperature >1406 K, the region in which the two stable compounds are AlNi and $AlNi_3$. In accordance with the Al–Ni phase diagram, compound $\alpha = BA_3$ and $\beta = AB$. This phase diagram has sufficient detail to correspond to realistic situations, and the basic ideas introduced here can be extended to more complicated systems.

As was done for the one-layer model, we define the following variables (see Figure 5b):

N'_B = amount (moles) of B in the melt
N'_A = amount (moles) of A in the melt
N_α = amount (moles) of α
N_β = amount (moles) of β
N_A = amount (moles) in the solid sphere of A
V_{mA} = molar volume of solid A
$V_{m\alpha}$ = molar volume of $\alpha = 4V_{mA}$
$V_{m\beta}$ = molar volume of $\beta = 2V_{mA}$
V_{mB} = molar volume of liquid B
a_1 = activity of B at interface I $\sim n_1$ = mole fraction at interface I
$a_{1,eq}$ = equilibrium activity of B at interface I $\sim n_{1,eq}$ = equilibrium mole fraction at interface I
a_2 = activity of B at interface II $\sim n_2$ = mole fraction at interface II
$a_{2,eq}$ = equilibrium activity of B at surface II $\sim n_{2,eq}$ = equilibrium mole fraction at interface II

a_3 = activity of B at interface III $\sim$ n_3 = mole fraction at interface III

$a_{3,eq}$ = equilibrium activity of B at surface III $\sim$ $n_{3,eq}$ = equilibrium mole fraction at interface III

D_1 = diffusion coefficient of B in the α phase

D_2 = diffusion coefficient of B in the β phase

J_1 = diffusion current at interface I

J_2 = diffusion current at interface II

J_3 = diffusion current at interface III

R_1 = reaction rate at interface I

R_2 = reaction rate at interface II

R_3 = reaction rate at interface III

As in the case of the one-layer model, we begin by specifying the rates of reaction at the interfaces:

interface I: $3A + B \rightleftharpoons \alpha$

$$\text{rate: } R_1 = k_1(n_1 - n_{1,eq}) \text{ (mol m}^{-2}\text{ s}^{-1}) \quad (17a)$$

interface II: $\alpha + 2B \rightleftharpoons 3\beta$

$$\text{rate: } R_2 = k_2(n_2 - n_{2,eq}) \text{ (mol m}^{-2}\text{ s}^{-1}) \quad (17b)$$

interface III: $\beta \rightleftharpoons$ melt

$$\text{rate: } R_3 = k_3(n_3 - n_{3,eq}) \text{ (mol m}^{-2}\text{ s}^{-1}) \quad (17c)$$

The diffusion coefficients, D_1 and D_2, and the rate constants, k_1, k_2, k_3, are assumed to have Arrhenius temperature dependence. The temperature profile, $T(t)$, is also chosen as in the case of one-layer model.

Because the reaction rates are assumed to be rapid and because a diffusional steady state is established, the total diffusional flux of B at each interface must balance the fluxes and the reaction in the interior interfaces. This condition leads to the equations:

$$r_3^2 J_3 = r_2^2 J_2 \quad (18a)$$

$$r_2^2 J_2 = r_2^2 (2R_2) + r_1^2 J_1 \quad (18b)$$

$$J_1 = R_1 \quad (18c)$$

i.e.,

$$r_3^2 J_3 = r_2^2 (2R_2) + r_1^2 R_1 \quad (19)$$

which shows that the flow of B at interface III is consumed by the reactions at the interfaces II and I. The equations for the amounts (moles) of each substance are

$$\frac{d}{dt}N_A = -(4\pi r_1^2)3R_1 \quad (20a)$$

$$\frac{d}{dt}N_\alpha = (4\pi r_1^2)R_1 - (4\pi r_2^2)R_2 \quad (20b)$$

$$\frac{d}{dt}N_\beta = (4\pi r_2^2)3R_2 - (4\pi r_3^2)R_3 \quad (20c)$$

$$\frac{d}{dt}N'_B = 4\pi r_3^2(-J_3 + R_3) = -(4\pi r_2^2)2R_2 - (4\pi r_1^2)R_1 + (4\pi r_3^2)R_3 \quad (20d)$$

$$\frac{d}{dt}N'_A = (4\pi r_3^2)R_3 \quad (20e)$$

where we have used eq 19 to obtain eq 20d.

Conservation of the total amount of A in the different phases requires

$$\frac{d}{dt}(N'_A + N_\beta + 3N_\alpha + N_A) = 0 \quad (21)$$

Similarly, conservation of the total amount of B requires

$$\frac{d}{dt}(N'_B + N_\beta + N_\alpha) = 0 \quad (22)$$

It is easy to see that the set of eqs 20 satisfies the required conservation of the total amount of A and B.

To relate eq 20 to the geometry of the reacting sphere and the time evolution of the layers of the intermetallic compounds, α and β, we need to write the equations of the system in terms of r_1, r_2, r_3, N'_A, and N'_B. This can be done by noting that

$$N_A = \frac{4\pi}{3} r_1^3 \frac{1}{V_{mA}}$$

$$N_\alpha = \frac{4\pi}{3}(r_2^3 - r_1^3)\frac{1}{V_{m\alpha}}$$

and

$$N_\beta = \frac{4\pi}{3}(r_3^3 - r_2^3)\frac{1}{V_{m\beta}} \quad (23)$$

Substituting these in the set of eqs 20 we obtain

$$\frac{dr_1}{dt} = -V_{mA}3R_1 \quad (24)$$

$$\frac{1}{V_{m\alpha}}\left(r_2^2\frac{dr_2}{dt} - r_1^2\frac{dr_1}{dt}\right) = r_1^2 R_1 - r_2^2 R_2 \quad (25)$$

$$\frac{1}{V_{m\beta}}\left(r_3^2\frac{dr_3}{dt} - r_2^2\frac{dr_2}{dt}\right) = r_2^2 3R_2 - r_3^2 R_3 \quad (26)$$

$$\frac{d}{dt}N'_B = -4\pi r_2^2 2R_2 - 4\pi r_1^2 R_1 + 4\pi r_3^2 R_3 \quad (27)$$

$$\frac{d}{dt}N'_A = 4\pi r_3^2 R_3 \quad (28)$$

In eq 25, we can eliminate dr_1/dt using eq 24 to obtain

$$\frac{dr_2}{dt} = \frac{r_1^2}{r_2^2}(V_{m\alpha} - 3V_{mA})R_1 - V_{m\alpha}R_2 \quad (29)$$

The first term on the right-hand side represents the change in r_2 due to change in volume when A converts to α upon reacting with B. We can use eq 29 to eliminate dr_2/dt in eq 26 and express the time derivative of r_3 as a function of the reaction rates.

$$\frac{dr_3}{dt} = \frac{r_1^2}{r_3^2}(V_{m\alpha} - 3V_{mA})R_1 + \frac{r_2^2}{r_3^2}(3V_{m\beta} - V_{m\alpha})R_2 - V_{m\beta}R_3 \quad (30)$$

Once again, we note that the first two terms on the right-hand side of eq 31 give the change in r_3 due to the changes in volume due to the conversion of A to α and α to β.

Equations 24 and 27−30 are a set of equations in r_1, r_2, r_3, N'_A, and N'_B. Our next task is to make these a set of closed

equations in which the reaction rates, R_k, are functions of r_1, r_2, r_3, N'_A, N'_B, and parameters in the system such as $n_{1,eq}$, $n_{2,eq}$, D_1, D_2, etc., which we shall refer to as system variables. To this end, we note the following:

$$R_3 = k_3(n_3 - n_{3,eq}) \tag{31}$$

in which

$$n_3 = \frac{N'_B}{N'_B + N'_A}$$

To express R_2 in terms of the system variables, we use the relations 18 for steady-state diffusion. As already noted, these relations tell us that, at steady state, the total amount of B entering each interface balances the amount of B being consumed by the reactions at interior interfaces. Furthermore, at a steady state,

$$J_1 = W_{12}(n_2 - n_1) \tag{32}$$

in which

$$W_{12} = D_1 \frac{r_2}{r_1} \frac{1}{r_2 - r_1}$$

and

$$J_2 = W_{23}(n_3 - n_2)$$

in which

$$W_{23} = D_2 \frac{r_3}{r_2} \frac{1}{r_3 - r_2} \tag{33}$$

From eq 18b, we get

$$2R_2 = J_2 - \frac{r_1^2}{r_2^2} J_1$$

Now, noting $R_2 = k_2(n_2 - n_{2,eq})$ and using eq 33 for J_2, we obtain

$$2k_2(n_2 - n_{2,eq}) = W_{23}(n_3 - n_2) - \frac{r_1^2}{r_2^2} J_1 \tag{34}$$

As we did for the one-layer model, we will show below that

$$J_1 = R_1 = \frac{k_1 W_{12}}{k_1 + W_{12}}(n_2 - n_{1,eq}) \tag{35}$$

Using this expression, eq 35, in eq 34, we obtain

$$2k_2(n_2 - n_{2,eq}) = W_{23}[(n_3 - n_{2,eq}) - (n_2 - n_{2,eq})] - \Gamma[(n_2 - n_{2,eq}) - (n_{1,eq} - n_{2,eq})] \tag{36}$$

in which

$$\Gamma = \frac{r_1^2}{r_2^2} \frac{k_1 W_{12}}{k_1 + W_{12}} \tag{37}$$

Collecting the term $(n_2 - n_{2,eq})$ on both sides,

$$(2k_2 + W_{23} + \Gamma)(n_2 - n_{2,eq}) = W_{23}(n_3 - n_{2,eq}) + \Gamma(n_{1,eq} - n_{2,eq})$$

$$(n_2 - n_{2,eq}) = \frac{W_{23}(n_3 - n_{2,eq}) + \Gamma(n_{2,eq} - n_{1,eq})}{2k_2 + W_{23} + \Gamma} \tag{38}$$

Thus, the reaction rate R_2 can be expressed as

$$R_2 = k_2(n_2 - n_{2,eq}) = k_2 \frac{W_{23}(n_3 - n_{2,eq}) + \Gamma(n_{2,eq} - n_{1,eq})}{2k_2 + W_{23} + \Gamma} \tag{39}$$

Finally, to express the reaction rate R_1 in terms of the system variables and derive eq 33, we note that at steady state, $R_1 = J_1$. Then, using eq 32 and $R_1 = k_1(n_1 - n_{1,eq})$, we obtain

$$k_1(n_1 - n_{1,eq}) = W_{12}(n_2 - n_1) = W_{12}[(n_2 - n_{1,eq}) - (n_1 - n_{1,eq})]$$

Collecting $(n_1 - n_{1,eq})$ terms, we arrive at

$$(n_1 - n_{1,eq}) = \frac{W_{12}}{k_1 + W_{12}}(n_2 - n_{1,eq})$$

Thus,

$$R_1 = k_1(n_1 - n_{1,eq}) = k_1 \frac{W_{12}}{k_1 + W_{12}}(n_2 - n_{1,eq})$$

which is precisely eq 35. Here, n_2 is expressed in terms of the system variables using eq 38.

$$n_2 = n_{2,eq} + \frac{W_{23}(n_3 - n_{2,eq}) + \Gamma(n_{2,eq} - n_{1,eq})}{2k_2 + W_{23} + \Gamma}$$

Thus, all the terms in the set of eqs 24 and 27−30 can be expressed in terms of the system variables. We gather all these terms and summarize the equations of the system that describe a two-layer model.

In summary, we have the following set of equations for the two-layer model: D_1, D_2, k_1, k_2, k_3, $n_{1,eq}$, $n_{2,eq}$, and $n_{3,eq}$ are given as Arrhenius functions of T; these and r_1, r_2, r_3, N'_A, and N'_B, are *the system variables*. The following functions of the system variables are then defined.

$$W_{12} = D_1 \frac{r_2}{r_1} \frac{1}{r_2 - r_1} \tag{40a}$$

$$W_{23} = D_2 \frac{r_3}{r_2} \frac{1}{r_3 - r_2} \tag{40b}$$

$$\Gamma = \frac{r_1^2}{r_2^2} \frac{k_1 W_{12}}{k_1 + W_{12}} \tag{40c}$$

$$n_3 = \frac{N'_B}{N'_B + N'_A} \tag{40d}$$

$$n_2 = n_{2,eq} + \frac{W_{23}(n_3 - n_{2,eq}) + \Gamma(n_{2,eq} - n_{1,eq})}{2k_2 + W_{23} + \Gamma} \tag{40e}$$

Reaction rates are

$$R_3 = k_3(n_3 - n_{3,eq}) \tag{41a}$$

$$R_2 = k_2 \frac{W_{23}(n_3 - n_{2,eq}) + \Gamma(n_{2,eq} - n_{1,eq})}{2k_2 + W_{23} + \Gamma} \tag{41b}$$

$$R_1 = k_1 \frac{W_{12}}{k_1 + W_{12}}(n_2 - n_{1,eq}) \tag{41c}$$

The above variables are used in the kinetic equations for the radii of the layers and the composition of the solution of A in B that surrounds the reacting layered sphere.

$$\frac{d}{dt}N'_B = -4\pi {r_2}^2 2R_2 - 4\pi {r_1}^2 R_1 + 4\pi {r_3}^2 R_3 \tag{42a}$$

$$\frac{d}{dt}N'_A = 4\pi {r_3}^2 R_3 \tag{42b}$$

$$\frac{d}{dt}r_3 = \frac{{r_1}^2}{{r_3}^2}(V_{m\alpha} - 3V_{mA})R_1 + \frac{{r_2}^2}{{r_3}^2}(3V_{m\beta} - V_{m\alpha})R_2 - V_{m\beta}R_3 \tag{42c}$$

$$\frac{d}{dt}r_2 = \frac{{r_1}^2}{{r_2}^2}(V_{m\alpha} - 3V_{mA})R_1 - V_{m\alpha}R_2 \tag{42d}$$

$$\frac{d}{dt}r_1 = -V_{mA}3R_1 \tag{42e}$$

In the following section, we solve the set of nonlinear equations (42) numerically to obtain the evolution of r_1, r_2, r_3, and the composition of the melt, N'_A, and N'_B.

IV. Numerical Study of the Two-Layer Model

In order to obtain realistic values of the layer growth, we use the extensively studied Al−Ni system as our model. As explained in detail below, available data for this system was used for numerical simulation, and when good physical data are not available, we make reasonable assumptions so as to have a physically meaningful results. Our model specifies experimental input needed for predicting the time-varying composition of system.

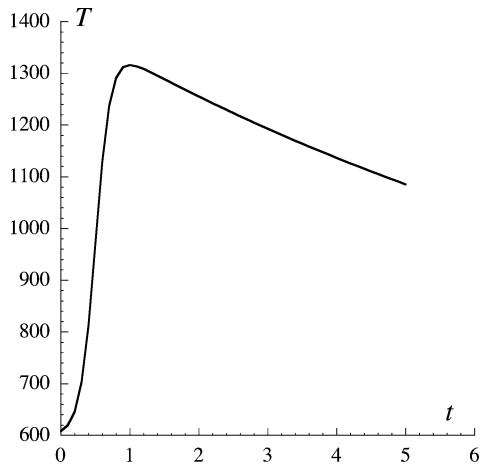

Figure 6. Temperature profile that the system is subjected to in the simulation. Component B melts at 933 K and A melts at 1728 K. This temperature simulates a condition in which particles of A are surrounded by liquid B. The temperature is measured in degrees K, and time, in seconds.

TABLE 1: Numerical Values of Parameters Used in the Model

	at. wt, g/mol	T_m, K	ρ (25 °C), g/cm ^{3}	V_m, m^3/mol
B (Al)	26.98	933	2.70	9.99×10^{-6}
A (Ni)	58.69	1728	8.90	6.59×10^{-6}

We use the following standard data[36] of Al and Ni for the components B and A, respectively (see Table 1).

For the equilibrium values of the mole fractions $n_{1,eq}$ and $n_{2,eq}$ (which are approximated to be the activities), we use the temperature-dependent molar Gibbs energies (per gram atom) of formation of the intermetallic compounds AlNi and $AlNi_3$ reported by Garg et al.[37] These energies are expressed as

$$\Delta G_f(X) = N_X[a + bT + cT\log_{10}(T)] \tag{43}$$

in which N_X is the number of atoms in the compound. $\alpha(AlNi_3)$: $N_X = 4$, $a = -32449.5$; $b = -70.5632$; $c = 22.4901$. β(AlNi): $N_X = 2$, $a = -46715.2$; $b = -139.944$; $c = 43.9741$. To compute the equilibrium values of the mole fractions (activities) of B for the reaction $B + 3A \rightleftharpoons BA_3$, which occurs at the interface I, for example, we consider the reaction

$$Al(\text{in } AlNi_3 \text{ phase}) + 3Ni(s) \rightleftharpoons AlNi_3(s)$$

which corresponds to

$$B(\text{in } \alpha \text{ phase}) + 3A(s) \rightleftharpoons BA_3(s)$$

At equilibrium,

$$\frac{a_{\alpha,eq}}{a_{B,eq}{a_{A,eq}}^3} = \exp(-\Delta G_{rxn}/RT) \tag{44}$$

If the activities $a_{\alpha,eq}$ and $a_{A,eq}$ and ΔG_{rxn} are known, then $a_{B,eq}$ can be calculated using this expression. By approximating the activities of the pure solids A and α to equal 1 and the activity of B in the α phase by the mole fraction, $n_{1,eq}$, we can obtain an approximate value of equilibrium mole fraction, $n_{1,eq}$, from eq 44 as a function of T. The equilibrium mole fraction, $n_{2,eq}$, is similarly estimated.

The equilibrium value of the mole fraction of B, $n_{3,eq}$, needed for the dissolution kinetics of the β layer into the melt, can be obtained from the phase diagram. For the assumed phase diagram of our system, the temperature dependence of the B mole fraction in the melt could be approximated by a function such as $a_{3,eq} = 0.8 - \exp(25000/RT)$.

In the literature, the diffusion coefficient is defined in different ways. Usually, the diffusion current is expressed in terms of the concentration gradient (following the Fick's law), and the corresponding diffusion coefficient which we shall denote as D_N has units of m^2 s^{-1}. However, a proper thermodynamic formulation indicates that the diffusion current is proportional to the gradient of chemical potential. Accordingly, the following expression for the diffusion current of the diffusing species B defined in terms of the gradient of chemical potential,

$$J_B = -D_\mu \frac{n}{V_m}\frac{\partial \ln a_B}{\partial r} \tag{45}$$

in which a_B is the activity of B, n the mole fraction of the diffusing species, B, and V_m is the molar volume of the medium in which B is diffusing. In dilute solutions, concentration is $c = n/V_m$ (mol m^{-3}). Hence, Fick's law in terms of n is

$$J_B = -D_N\frac{\partial c}{\partial r} = -\frac{D_N}{V_m}\frac{\partial n}{\partial r} \tag{46}$$

D_μ in eq 45 and D_N in eq 46 have the same units, m^2 s^{-1}. If we set activity $a_B \sim n$, then $D_\mu = D_N$. In eq 46, the quantity (D_N/

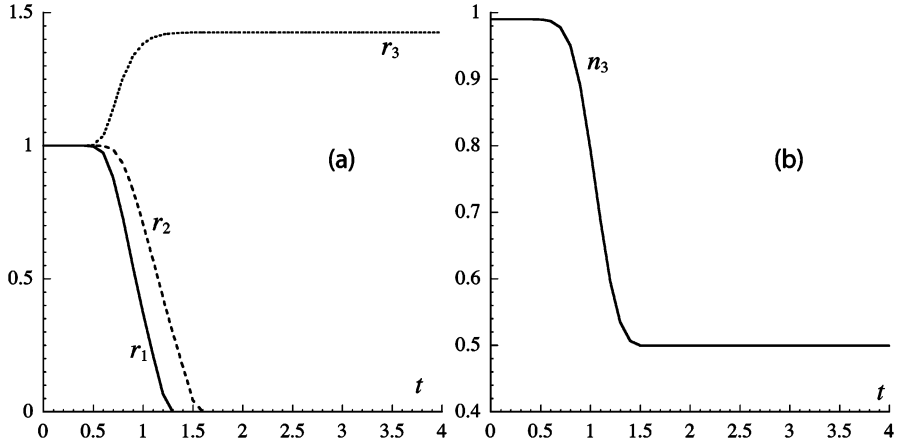

Figure 7. Evolution of (a) layer radii, r_1, r_2, and r_3 and (b) n_3, the mole fraction of B in the melt. In this simulation $D_1 = 6.0 \times 10^{-8} \exp(-8.9 \times 10^4/RT)$ and $D_2 = 1.0 \times 10^{-8} \exp(-8.9 \times 10^4/RT)$. The radii are measured in micrometers, and time, in seconds.

V_m) has the units (mol m^{-1} s^{-1}). In some articles, the "diffusion coefficient" is expressed in these units. In an article by Hibino,[23] for example, the following diffusion coefficient was used for diffusion of Al in Ni_2Al_3.

$$D = 1.2 \times 10^{-3} \exp(-89000/RT) \text{ mol m}^{-1} \text{ s}^{-1} \quad (47)$$

In this case $D_\mu = D_N = DV_m$. Since the molar volume of Ni_2Al_3 is $\sim 5 \times 10^{-5}$ m^3 mol^{-1}, we have the approximate value

$$D_N = 5 \times 10^{-5} \times 1.2 \times 10^{-3} \exp(-89000/RT) \text{ m}^2 \text{ s}^{-1}$$
$$= 6.0 \times 10^{-8} \exp(-89000/RT) \text{ m}^2 \text{ s}^{-1} \quad (48)$$

In our numerical simulations, as specified below, we use these approximate values for diffusion of B in the different phases.

The rate constants for the reactions at the interfaces I and II are difficult to estimate. For the reaction $2Ni + 3Al \rightleftharpoons Ni_2Al_3$, which occurs at the interface of Ni and the Ni_2Al_3, Hibino[23] estimates the reaction rate constant as

$$k = 1.35 \times 10^4 \exp(120000/RT) \text{ mol m}^{-2} \text{ s}^{-1} \quad (49)$$

We approximate the value for the rate constants k_1 and k_2 at interfaces I and II close to this value.

The dissolution of the outermost layer can be modeled with diffusion of the solid into the liquid. The dissolution of Ni into Al is through diffusion whose activation energy was found to be 17.9 ± 2.9 kcal mol^{-1} $= 74.82 \pm 11.9$ kJ mol^{-1}.[24] Thus, for the dissolution of the β-layer into the liquid, an Arrhenius coefficient can be used. Gennari et al.[24] use the following for the diffusion coefficient:

$$D = D_0 \exp(-\epsilon/RT) \quad (50)$$

in which

$$\epsilon = 76 \text{ kJ mol}^{-1}, \quad D_0 = 10^{-4} \text{ m}^2 \text{ s}^{-1}$$

Hence, for the rate of dissolution at the interface of the outermost β-layer into the surrounding liquid B, we may use

$$\text{rate} = k_0 \exp(-76000/RT)(n_3 - n_{3,eq}) = k_3(n_3 - n_{3,eq}) \quad (51)$$

in which k_0 is a parameter whose value can be adjusted in the model. In the numerical results shown below, $k_0 = 20$ mol m^{-2} s^{-1}. As β layer dissolves in B, the mole fraction of B decreases and the solution approaches the dissolution equilibrium. The

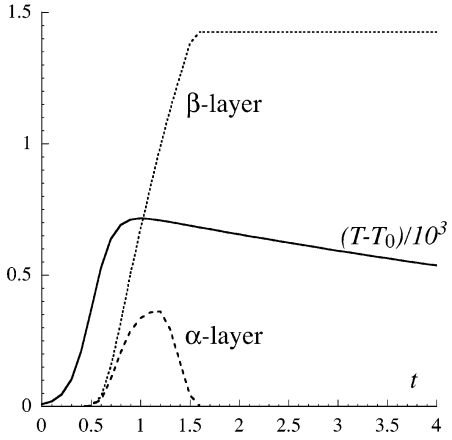

Figure 8. Evolution of the thickness of the α-layer, $(r_2 - r_1)$, the β-layer, $(r_3 - r_2)$, and the system temperature. The time evolution of T is simulated using expression 1, in which $T_0 = 600$, $C = 800$, $D = 100$, $c = 9$, and $d = 9.1$. In this simulation, $D_1 = 6.0 \times 10^{-8} \exp(-8.9 \times 10^4/RT)$ and $D_2 = 1.0 \times 10^{-8} \exp(-8.9 \times 10^4/RT)$. The radii are measured in micrometers, and time, in seconds.

mole fraction, $n_{3,eq}$, at which the equilibrium is reached can be obtained from the phase diagram (point 7 in Figure 5a). As stated above, we use $n_{3,eq} = a_{3,eq} = 0.8 - \exp(25000/RT)$.

The temperature profile the system is subjected to in our simulations is shown in Figure 6. The temperature rapidly reaches a maximum of $\sim$1300 K and slowly decreases, as is the case in many SHS systems. This temperature profile is obtained using expression 1, in which $T_0 = 600$, $C = 800$, $D = 100$, $c = 9$, and $d = 9.1$. The initial size of particles of A is assumed to be $r_0 = 1.0$ μm, and all the plots of layer radii are in units in which $r_0 = 1.0$. The initial amounts (moles) of A and B are assumed to be equal. For the diffusion coefficients, we consider two cases: one in which $D_1 > D_2$ and the other one in which $D_2 > D_1$. Figure 7 shows the evolution of the layer radii for the case $D_1 > D_2$ and the evolution of the mole fraction, n_3, of B in the solution phase outside the reacting solid sphere, which is initially A. The value of n_3 levels off at 0.5 because, even though the dissolution of the β-layer seizes at n_3 less than 0.5, the continued diffusion of B from the B-rich phase into the β-layer in the sphere results in the composition of the entire system being that of the β phase in which A and B are in equal amounts. The simulation shows that an entire particle of A is converted into α and β phases in $\sim$1.3 s, and by $\sim$1.5 s, the transformation to β phase is complete. Figure 8 shows

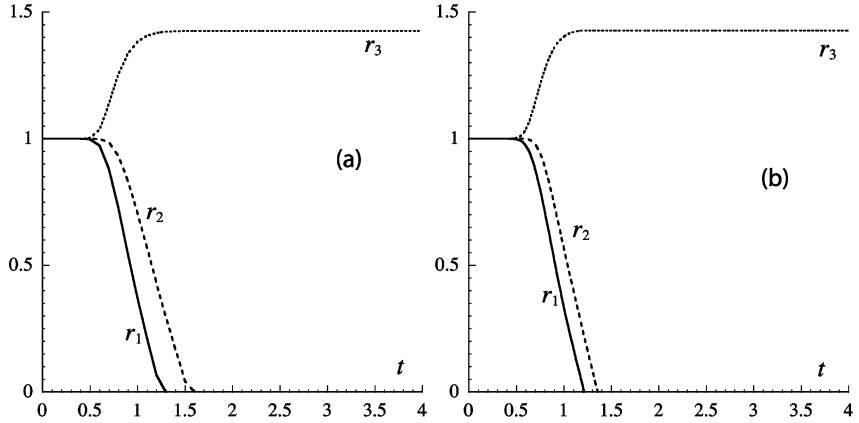

Figure 9. Comparison of the evolution of layer radii, r_1, r_2, and r_3 in the case when (a) $D_1 > D_2$: $D_1 = 6.0 \times 10^{-8} \exp(-8.9 \times 10^4/RT)$ and $D_2 = 1.0 \times 10^{-8} \exp(-8.9 \times 10^4/RT)$ and (b) $D_1 < D_2$: $D_1 = 1.0 \times 10^{-8} \exp(-8.9 \times 10^4/RT)$ and $D_2 = 6.0 \times 10^{-8} \exp(-8.9 \times 10^4/RT)$. The radii are measured in micrometers, and time, in seconds.

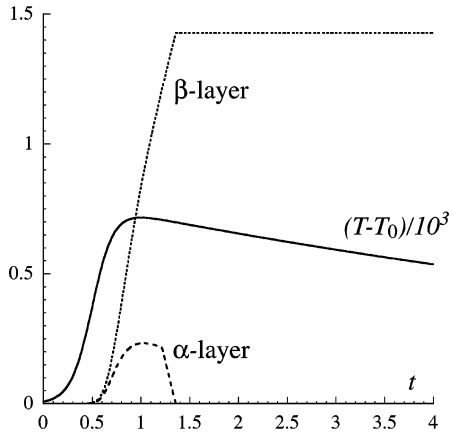

Figure 10. Evolution of the thickness of the α-layer, $(r_2 - r_1)$, the β-layer, $(r_3 - r_2)$, and the system temperature. The time evolution of T is simulated using expression 1, in which $T_0 = 600$, $C = 800$, $D = 100$, $c = 9$, and $d = 9.1$. In this simulation $D_1 = 1.0 \times 10^{-8} \exp(-8.9 \times 10^4/RT)$ and $D_2 = 6.0 \times 10^{-8} \exp(-8.9 \times 10^4/RT)$. The radii are measured in micrometers; time, in seconds; and the temperature increase, in degrees K.

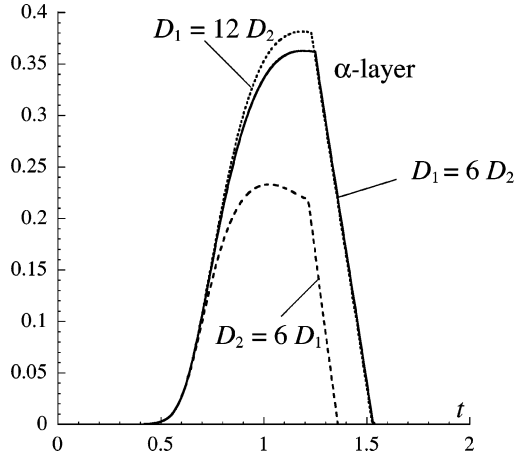

Figure 11. Comparison of the evolution of the α-layer thickness for various relative values of the diffusion coefficient of component B in the α-phase (D_1) and β phases (D_2). The radii are measured in micrometers, and time, in seconds.

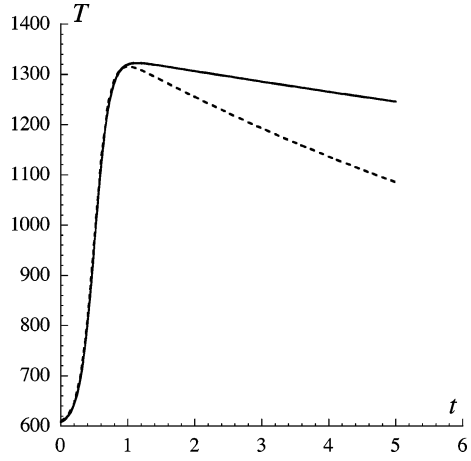

Figure 12. Varying the temperature profile using expression 1. The solid curve shows a lower cooling rate: $T_0 = 600$, $C = 750$, $D = 100$, $c = 9$, and $d = 9.03$. The dashed curve: $T_0 = 600$, $C = 800$, $D = 100$, $c = 9$, and $d = 9.1$. The temperature is measured in degrees K, and time, in seconds.

the evolution of the layer thickness and the temperature. As can be seen, the α-layer thickness increases, reaches its maximum close to the point at which T reaches its maximum and reduces to zero all in about 1 s. For an initial radius of 1 μm, the maximum thickness of the α layer is ~0.35 μm. The final sphere of the β phase has a radius of nearly 1.5 μm.

Figures 9 shows the evolution of the layer radii when $D_1 > D_2$ and when $D_1 < D_2$. There is no significant difference between the two cases up to a factor of 6 between the two diffusion coefficients (this is not to say that a larger difference may not result in a significant difference in the evolution of the layer radii r_1, r_2, and r_3). Figure 10 shows the evolution of the thickness of layers of the α- and the β-phases when $D_1 < D_2$. The dependence of the evolution of the α-layer thickness on the relative values the diffusion coefficients is shown in detail in Figure 11. The maximum thickness of the α-layer increases with an increase in D_1 relative to D_2. This analysis shows that the intermediate layers may act as a diffusionnal barrier for the progress of the reaction. In the case that D_1 is larger than D_2, the maximum size of the α-layer is reached in the cooling zone of the thermogram. In the opposite case ($D_1 < D_2$), the time scale of the overall process is slightly reduced, and the maximum size of the layer is reached when the temperature reaches the combustion temperature and the tickness of the layer is smaller. The diffusional transport in the intermediate layer will thus influence the morphology at the level of the individual grains.

Through the simulation, we can also see the effect of the temperature profile. In Figure 12, we show a temperature profile

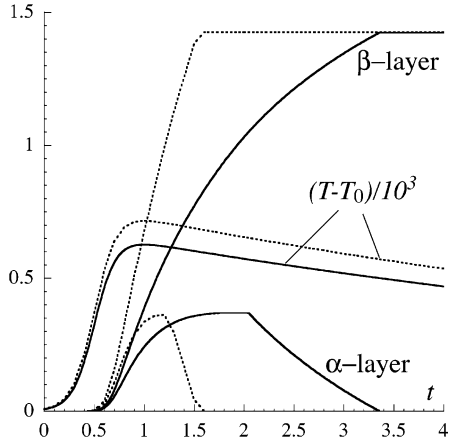

Figure 13. Comparison of the evolution of the thickness of the α-layer, ($r_2 - r_1$), and β-layer, ($r_3 - r_2$), when the system is subjected to temperature profiles that differ in the maximum value reached. The dotted and solid curves for the α- and β-layers correspond to the dotted and solid temperature curves obtained using expression 1. The solid curve shows a profile with a lower maximum temperature: $T_0 = 600$, $C = 700$, $D = 100$, $c = 9$, and $d = 9.1$. The dashed curve: $T_0 = 600$, $C = 800$, $D = 100$, $c = 9$, and $d = 9.1$. The radii are measured in micrometers; time, in seconds; and the temperature increase, in degrees K.

in which the system reaches the same maximum T but has a slower cooling rate. Under this temperature profile (diffusion coefficients are the same as those used in generating the data shown in Figure 7), we found that the evolution for the radii is essentially the same as that shown in Figure 7. However, when the temperature profile is changed so that the maximum value reached is lower, we find a significant difference in the evolution of the system. Figure 13 shows the temperature profile with a lower maximum and the corresponding evolution of the layer thicknesses. Since the temperature profile that each particle experiences depends on the geometry and the composition of the entire sample, it can be altered to have the desired properties (high maximum value, fast cooling rates, etc.).

From our analysis, it appears that the maximum temperature has a strong influence on the microstructural evolution. A seen in Figure 13, the process may be incomplete after the passage of the front when the combustion temperature is not high enough. This particular situation leads to an incomplete conversion of A that is surrounded by the α-layer, as may be observed in some experiments, or by quenching the sample. Since it is possible to control the combustion temperature by adding some diluent or by preheating the sample, the combustion temperature might be used as a control parameter to obtain alloys with a desired microstructure.

V. Concluding Remarks

The theory presented in this article is based on the phase diagram of the reacting compounds. It presents a way to understand the "microevolution" of the system on the level of a single particle. The procedure of obtaining a set of closed equations for one- and two-phase models outlined in Sections II and III can be extended to a larger number of phases, albeit with longer algebraic expression for the system equations. The model does not contain any parameters that cannot be experimentally obtained. On the other hand, by studying the predictions of this model more extensively, we will be able to identify those parameters that must be known with some accuracy and those whose values we need to know only approximately. For example, our simulations show that the relative values of the diffusion coefficients of B in the two phases are not very significant, but the maximum of the propagating temperature pulse is important.

In addition to the results presented in this article, our future investigations will identify conditions that lead to different final compositions, such as layered structures of different phases. The theory can also be extended to calculate the heat generated by the reaction in each particle if the relevant enthalpies are given. One could also envision a broader extension of this theory. In SHS, since the profile of the propagating temperature pulse itself depends on the enthalpy of the reacting components, a "self-consistent mean-filed theory" could be formulated. In this approach, initially, a time-varying mean temperature, $T_{in}(t)$, that each particle is subjected to is assumed. Using this temperature, the reaction enthalpy of each particle as a function of time, $H(t)$, is obtained. The reaction enthalpy of each particle, $H(t)$, is then used to obtain the temperature, $T_{out}(t)$, of the system using particle density, heat capacity, and other such relevant variables. Thus, each temperature function used as an input generates another temperature function as the output: $T_{in}(t) \rightarrow H(t) \rightarrow T_{out}(t)$. This process is repeated until there is good convergence or "self-consistency" between functions $T_{in}(t)$ and $T_{out}(t)$. Such an approach, which has proved highly useful in the study of many electron systems, might prove useful in the theory of SHS.

Appendix A

In spherical geometry, steady-state diffusion implies: $4\pi r^2 J = \text{const}$. As discussed in Section IV (see eqs 45 and 46), using the thermodynamic formulation of diffusion, we write the diffusion current in terms of the gradient of the mole fraction n. Since $J = -D_1 \partial n/\partial r$, we can solve for n to obtain $n = (C_1/r) + C_2$. Using the boundary conditions $n = n_1$ at r_1 and $n = n_2$ at r_2, we obtain

$$n_1 = (C_1/r_1) + C_2 \tag{A1}$$

$$n_2 = (C_1/r_2) + C_2 \tag{A2}$$

Solving eqs A1 and A2 for C_1 gives

$$C_1 = \frac{n_1 - n_2}{1/r_1 - 1/r_2} \tag{A3}$$

The current, J_1, can now be calculated.

$$J_1 = -D_1 \left.\frac{\partial n}{\partial r}\right|_{r=r_1} = \frac{D_1 C_1}{{r_1}^2} = D_1 \left(\frac{n_1 - n_2}{1/r_1 - 1/r_2}\right) \frac{1}{{r_1}^2} = -D_1 \frac{r_2}{r_1} \frac{n_2 - n_1}{r_2 - r_1} \tag{A4}$$

The negative sign implies that the current is flowing toward the center if $n_2 > n_1$. This gives eq 6, in which a positive J_1 is used for the flow toward the center.

Acknowledgment. We are grateful to Profs. J.-C. Niepce and F. Bernard for helpful discussions. This work has been supported in part by the Chemistry Department and the Centre de dynamique des systèmes complexes of the University of Burgundy and by Wake Forest University.

References and Notes

(1) Merzhanov, A. G. *J. Mater. Chem.* **2004**, *14*, 1779.
(2) Merzhanov, A. G. *Int. Chem. Eng.* **1980**, *20*, 150.

(3) Volpert, V. A.; Volpert, A. I.; Merzhanov, A. G. *Combust. Explos. Shock Waves (Engl. Transl.)* **1983**, *19*, 435.
(4) Munir, Z. A. *Ceram. Bull.* **1988**, *67*, 342.
(5) Rogachev, A. S. *Int. J. SHS* **1997**, *6*, 215.
(6) Subrahmanyam, J.; Vijayakumar, M. *J. Mater. Sci.* **1999**, *27*, 6249.
(7) Anselmi-Tamburini, U.; Munir, Z. A. *J. Appl. Phys.* **1989**, *66*, 5039.
(8) Clevenger, L. A.; Thompson, C. V.; Tu, K. N. *J. Appl. Phys.* **1990**, *67*, 2894.
(9) Alman, D. E.; Hawk, J. A.; Petty, A. V. Jr.; Rawers, J. C. *J. Met.* **1994**, *46*, 31.
(10) Alman, D. E.; Rawers, J. C.; Hawk *J. A. Metall. Mater. Trans. A* **1995**, *26*, 589.
(11) Dyer, T. S.; Munir, Z. A. *Metall. Mater. Trans. B* **1995**, *26*, 603.
(12) Zhu, P.; Li, J. C. M.; Liu, C. T. *Mater. Sci. Eng. A* **1997**, *239*, 532.
(13) Shteinberg, A. S.; Shcherbakov, V. A.; Munir Z. A. *Combust. Sci. Technol.* **2001**, *169*, 1.
(14) Biswas, A.; Roy, S. K. *Acta Mater.* **2004**, *52*, 257.
(15) Varma, A.; Rogachev, A. S.; Mukasyan, A. S.; Hwang, S. *Proc. Natl. Acad. Sci. U.S.A.* **1998**, *95*, 11053.
(16) Deevi, S. C. *Mater. Sci. Eng. A* **1992**, *149*, 241.
(17) Philpot, K. A.; Munir, Z. A.; Holt, J. B. *J. Mater. Sci.* **1987**, *22*, 159.
(18) Mukasyan, A. S.; Rogachev, S. A.; Varma, A. *Chem. Eng. Sci.* **1999**, *54*, 3357.
(19) Fan, Q.; Chai, H.; Jin, Z. *Intermetallics* **2001**, *9*, 609.
(20) Varma, A.; Kachelmyer, C. R.; Rogachev, A. S. *Int. J. SHS* **1996**, *5*, 1.
(21) Aleksandrov, V. V.; Korchagin, M. A. *Combust. Explos. Shock Waves* **1988**, *23*, 557.
(22) Kanury, A. M. *Metall. Trans. A* **1992**, *23*, 2349.
(23) Hibino, A. *Int. J. SHS* **1999**, *8*, 13.
(24) Gennari, S.; Maglia, F.; Anselmi-Tamburini, U.; Spinolo, G. *J. Phys. Chem. B* **2003**, *107*, 732.
(25) Arimondi, M.; Anselmi-Tamburini, U.; Gobetti, A.; Munir, Z. A.; Spinolo, G. *J. Phys. Chem. B* **1997**, *101*, 8059.
(26) Maglia, F.; Anselmi-Tamburini, U.; Gennari, S.; Spinolo, G. *Phys. Chem. Chem. Phys.* **2001**, *3*, 489.
(27) Maglia, F.; Anselmi-Tamburini, U.; Gennari, S.; Spinolo, G. *J. Phys. Chem. B* **2002**, *106*, 6121.
(28) Gennari, S.; Maglia, F.; Anselmi-Tamburini, U.; Spinolo, G. *Intermetallics* **2003**, *11*, 1355.
(29) Gennari, S.; Anselmi-Tamburini, U.; Maglia, F.; Spinolo, G.; Munir, Z. A. *Acta Mater.* **2006**, *54*, 2343.
(30) Wang, L. L.; Munir Z.A. *Metall. Mater. Trans. B* **1995**, *26*, 595.
(31) Karnatak, N.; Dubois, S.; Beaufort, M. F.; Vrel, D. *Int. J. SHS* **2003**, *12*, 197.
(32) Dumez, M.-C.; Marin-Ayral, R.-M.; Tédenac J.-C. *J. Alloys Compd.* **1998**, *268*, 141.
(33) Zhu, P.; Li, J. C. M.; Liu, C. T. *Mater. Sci. Eng.* **2002**, *A329*−*331*, 57.
(34) Kondepudi, D. K.; Prigogine, I. P. *Modern Thermodynamics: From Heat Engines to Dissipative Structures*; John Wiley: New York, 1998.
(35) Delmon, B. *Introduction a la cinétique hétérogene*; Editions Technip: Paris, 1969.
(36) *CRC Handbook of Physics and Chemistry*, 75th ed.; CRC Press: Boca Raton.
(37) Garg, S. P.; Kale, G. B.; Patil, R. V.; Kundu, T. *Intermetallics* **1999**, *7*, 901.